Synthesis of *Escherichia coli* OmpA oral nanoparticles and evaluation of immune function against the main pathogenic bacteria of cow mastitis

Xiang Liu
Northwest A&F University
Wei Sun
Shaanxi University of Technology
Nana Wu
Shaanxi University of Technology
Na Rong
Shaanxi University of Technology
Chao Kang
Shaanxi University Technology
Sijie Jian
Shaanxi University of Technology
Chunlin Chen
Shaanxi University of Technology
Chen Chen (cchen@snut.edu.cn)
Shaanxi University of Technology
Xiaoying Zhang
Northwest A&F University

Research

Keywords: E. coli, cow mastitis, OmpA protein nanoparticles, immune function, oral vaccine

Posted Date: February 18th, 2021

DOI: https://doi.org/10.21203/rs.3.rs-202054/v1

Abstract

Background: *Escherichia coli* is a main pathogenic bacteria that causes cow mastitis, a condition that results in huge economic losses. There is lack of orally delivered prevention for cow mastitis. The outer membrane protein A (OmpA) of *E. coli* is immunogenic and can be used in a vaccine. In the present study, OmpA was synthesized into nanoparticles (NP-OmpA) for oral delivery and prevention of cow mastitis.

Methods: OmpA was purified with Ni-NTA flow resin and encapsulated with chitosan (CS) to prepare NP-OmpA nanoparticles. The gastrointestinal tract was simulated *in vitro* (PBS, pH 1.2) to measure the protein release rate. The optimal preparation conditions for NP-OmpA were determined by analyzing the concentrations of OmpA and CS, magnetic mixing speed, mixing time, and ratio of tripolyphosphate (TPP)/CS (W/W). NP-OmpA safety was detected by function factors and histopathological examination of livers and kidneys. Immune activity of NP-OmpA was determined using qRT-PCR to detect immune-related gene expression, leukocyte phagocytosis of *Staphylococcus aureus*, ELISA to detect antiserum titer and immune recognition of *E. coli*, and the organ index. The immune protection function of NP-OmpA was assessed by the protection rate of NP-OmpA to *E. coli* in mice, qRT-PCR for inflammation-related gene expression, assay kits for antioxidant factors, and visceral injury in the histopathological sections.

Results: NP-OmpA nanoparticles had a nanodiameter of about 700 nm, loading efficiency (LE) of 79.27%, and loading capacity (LC) of 20.31%. The release rate was less than 50% *in vitro*. The optimal preparation conditions for NP-OmpA were OmpA protein concentration of 2 mg/mL, CS concentration of 5 mg/mL, TPP/CS (W/W) of 1:1, magnetic mixing speed of 150 r/min, and mixing time of 15 min. Histopathological sections and factors of uric acid (UA), creatinine (Cr), alanine aminotransferase (ALT), aspartate transaminase (AST), catalase (CAT), glutathione (GSH), and malondialdehyde (MDA) showed NP-OmpA was safe for mice liver and kidney. NP-OmpA could enhance the immune-related gene expression of IFN-γ and HSP70 in the spleen, liver, and kidney, and the leukocyte phagocytosis of *S. aureus*. The antiserum titer (1: 3200) was obtained from mice immunized with NP-OmpA, which had an immune recognition effect to *E. coli*. The immune protection rate of NP-OmpA was 71.43% ($p < 0.05$) to *E. coli*. NP-OmpA could down regulate the inflammation-related gene expression of TNF-a, IL-6, and IL-10 in the spleen, liver, and kidney, and the antioxidant factors MDA and SOD in the liver, and reduce the injury in mice liver and kidney induced by *E. coli*.

Conclusion: A novel NP-OmpA nanoparticle was synthesized, and the optimal preparation conditions were determined. The nanoparticles were found to be safer and have better immune function. They are expected to induce a response that resists infection with the main pathogenic bacteria (*E. coli*) of cow mastitis.

Background

Escherichia coli is a gram-negative bacterium that widely exists in the natural environment and can enter the animal body through the skin or digestive tract [1]. It is one of the main pathogenic bacteria that

causes dairy cow mastitis, which results in huge economic losses in the dairy industry [2, 3]. It can also induce diseases such as septicemia, pericarditis, aerocyst, ophthalmia, and omphalitis in chickens [4, 5], and causes hemolytic uremia, neonatal septicemia, and meningitis in humans [6-8]. Thus, *E. coli* is an opportunistic zoonotic pathogen. At present, antibiotics are the most common drugs used to prevent and treat *E. coli* infection. However, the abuse of antibiotics will inevitably lead to bacterial resistance, drug residues, and environmental pollution, and also affect the microecological balance of animal intestinal flora [9, 10]. It is therefore necessary to develop new drugs to prevent and treat *E. coli* infection.

Outer membrane protein A (OmpA) is the main outer membrane protein (OMP) of gram-negative bacteria. It consists of an N-terminal transmembrane domain (1–171) and a C-terminal cytoplasmic domain (172–325) and is genetically highly conserved. OmpA plays an important role in biofilm formation, host cell invasion, pore formation, and multidrug resistance [11]. More specifically, *E. coli* OmpA plays a key role in pathogenicity and is the main virulence factor in *E. coli* infection [12]. OmpA also has strong immunogenicity and can induce innate and adaptive immune responses in animal hosts. OmpA can regulate the expression of cytokines, chemokines, nitric oxide synthase, and cyclooxygenase-2, and protect mice from death caused by *E. coli* infection [13]. Anti-OmpA antibodies can regulate the function of specific phagocytosis to protect against *E. coli* infection [14]. We found that OmpA had significant protective rates of 58.33% and 46.15% against *E. coli* and *Staphylococcus aureus,* respectively, the pathogenic bacteria of cow mastitis, and that the OmpA fragment is also immunogenic [15]. Therefore, OmpA is a vaccine candidate for the prevention of *E. coli* infection.

To further improve the immune function of OmpA and produce a formulation that could survive degradation in the gastrointestinal tract, achieve sustained release, and have enhanced efficacy, we used a nano preparation method to encapsulate OmpA with chitosan (CS) to synthesize nanoparticles.

Materials And Methods

Animals and bacterial strains

Kunming mice (4 weeks old) were purchased from Chongqing Tengxin Biotechnology Co. Ltd., China. All animal procedures were performed in accordance with the guidelines prescribed in the Guide for the Care and Use of Laboratory Animals, and were approved by the Animal Ethics Committee of the Shaanxi University of Technology, China (No. 2019-015).

E. coli and *S. aureus* isolated from cow mastitis and the *E. coli* OmpA expression strain were all preserved in the biochemistry and molecular laboratory of Shaanxi University of Technology.

Expression, purification, and preparation of nanoparticles of OmpA

Expression and purification of OmpA were performed as described previously [16]. Briefly, the OmpA expression strain was cultured overnight and transferred to 600 mL LB medium until OD_{600} nm = 0.5. Isopropyl-β-D-thiogalactoside (IPTG) was then added and induced at 20℃ for 24 h. Bacterial cells were

harvested by centrifugation and disrupted by sonication with an ice bath. Finally, OmpA was purified with the Ni-NTA flow resin (Sigma, USA).

The OmpA nanoparticles (NP-OmpA) were prepared by CS encapsulation. Briefly, TPP (3 mL, 1 mg/mL) was added dropwise to a CS solution (10 mL, 1 mg/mL), and stirred for 10 min at 700 r/min. After centrifugation (15 min at 9,500 r/min), the precipitate was added to 25 mL of water and subject to ultra sound (2 min at 50% power). Then 3 mL of OmpA was added dropwise. After centrifugation, 10 mL of water was added to the precipitate to obtain the NP-OmpA. Nanoparticle diameter and zeta potential were analyzed using a Laser Particle Size Analyzer (Beckman, USA), and the morphology was observed using a scanning electron microscope (Phenom Pro, Netherlands) [17].

In vitro release of NP-OmpA

NP-OmpA was tested for *in vitro* protein release to simulate the digestive function of the gastrointestinal tract. Briefly, the NP-OmpA solution was transferred to a dialysis bag (MW 14–20 kDa) that was placed into the pH 1.2 solution. At each assigned time point (0, 2, 4, 6, 8, 10, 12, 14, 16, 18, 20, 22, 24, 36, 48, 60, 72, 84, and 96 h), 200 μL of supernatant was taken from the solution and analyzed for protein content using Bradford diagnostic kits [18].

The optimal preparation conditions for NP-OmpA

Nanoparticles were prepared as described by Li et al. [17], with minor modifications. The factors that were optimized for the preparation of the NP-OmpA were the concentrations of OmpA and CS, magnetic mixing speed, mixing time, and the ratio of TPP/CS (W/W). Each is briefly described here. (1) The concentration of OmpA: TPP (3 mL, 0.5 mg/mL) was added dropwise into a CS solution (10 mL, 0.5 mg/mL) with stirring for 10 min at 700 r/min. After centrifugation (15 min at 9,500 g), 25 mL of water was added to the precipitate under continuous ultrasonication for 2 min, and 3 mL OmpA solution (0.5, 1.0, 1.5, 2.0, 2.5 mg/mL) was added dropwise with stirring (150 r/min for 15 min). After centrifugation (15 min at 9,500 r/min), nanoparticles were obtained. (2) The concentration of CS: TPP was added into the CS solution (1.0, 2.0, 3.0, 4.0, and 5.0 mg/mL), and mixing (10 min at 700 r/min). After centrifugation, 25 mL of water was added to the precipitate under continuous ultrasonication, and 3 mL of OmpA solution was added. Finally, nanoparticles were obtained by centrifugation. (3) The ratio of TPP/CS: TPP was added into the CS solution at the ratios of TPP/CS (W/W) of 1:1, 1:2, 1:3, 1:4, and 1:5. After centrifugation, the precipitate was re-suspended and OmpA solution was added. Finally, nanoparticles were obtained by centrifugation. (4) Magnetic mixing speed: After centrifugation, the precipitate was re-suspended with dH_2O, and OmpA solution was added dropwise with magnetic mixing speed at 100, 150, 300, 500, or 700 r/min. Finally, nanoparticles were obtained by centrifugation. (5) Mixing time: After centrifugation, the precipitate was re-suspended and OmpA solution was added with mixing times of 10, 15, 20, 30, 60, and 120 min. Finally, nanoparticles were obtained by centrifugation. Also, loading efficiency (LE), loading capacity (LC), and particle diameter were measured to determine the optimal factors for preparation of NP-OmpA.

Immunoprotective effect of NP-OmpA

Kunming mice were divided into four groups with 20 mice in each group. Groups 1 and 2 were vaccinated with NP-OmpA and OmpA, respectively. Group 3 was vaccinated with CS nanoparticles without OmpA (NP-Empty), while Group 4 received normal saline (NC). All vaccines were orally administered at 6 μg/g of mice body weight four times. The first immune interval was 14 days, and the subsequent immune interval was 7 days. Mice were challenged 7 days post-vaccination with *E. coli*, and mouse mortality was counted after 15 days. At that point, the immune protection rate (RPS) of the mice was calculated, RPS (%) =1- (% vaccinated mortality/% control mortality) × 100. SPSS software was used to test statistical significance [19].

Organ index, white blood cell (WBC) count, and leukocyte phagocytosis

The organ index was implemented as follows: the mice were weighed after cervical dislocation. The spleen and thymus were removed and weighed. The organ index = organ weight / mice weight.

WBC counts were conducted as follows: mice anticoagulant was collected to prepare blood smears. Wright's and Giemsa's dye solutions were used for staining, and samples were washed slowly for 3 min with water. After drying, microscopic counting was performed.

Leukocyte phagocytosis was performed as described previously [20]. Briefly, 0.2 mL of mice anticoagulant was added to 2 mL of *S. aureus* (6×10^8 CFU/mL) and shaken for 60 min at 25℃ in a water bath. The mixed liquid smears were drawn with a pipette. Each sample was fixed with methanol for 3–5 min, stained (Giemsa) for 30 min, washed and air dried, and then observed by oil microscope. Phagocytic percentage (*PP* %) = no. of WBCs involved in phagocytosis per 100 leukocytes / 100 ×100%. Phagocytic index (*PI* %) = no. of bacteria phagocytized / no. of WBCs phagocytizing bacteria. The results were analyzed by variance analysis (ANOVA) and the Tukey test ($P < 0.05$) with SPSS 19.0 software.

Detection of the interaction between the antiserum and *E. coli*, and the antiserum titer

Interaction between the antiserum and bacteria was assessed by ELISA as described previously [19]. Briefly, after *E. coli* were harvested, 1% oxymethylene (W/V) was added for 90 min at 80°C to inactivate the bacteria, and the solution was adjusted until OD_{600} nm = 0.2. The bacterial solution was transferred to 1.5 mL tubes, and antisera at various dilutions were added before incubation for 1 h at 37°C. After washing with PBS, rabbit anti-mouse antibody (Sigma, USA) was added, and the solution was washed with PBS again. The bacteria were suspended with 20 μL of PBS and transferred to an enzyme-linked plate. Coloration liquid (50 μL H_2O_2 and 50 μL TMB) and stop solution (50 μL 2M H_2SO_4) were added to the wells, and absorbance was read at OD_{450} nm with a microplate reader (Bio-Rad, USA).

Serum antibody titer was detected by ELSA as described previously [19]. Briefly, the purified OmpA was added to an enzyme-linked plate and incubated with blocking solution (5% skim milk), and various dilutions of antiserum were added before incubation for 1 hour at 37°C. After washing, rabbit anti-mouse

antibody (Sigma, USA) was added to the plate. Coloration liquid (50 μL H_2O_2 and 50 μL TMB) was added to each well and the absorbance read at OD_{450} nm with a microplate reader (Bio-Rad, USA).

Biochemical indexes for physiological function of visceral organs

Four-week-old mice were divided into six groups. Groups 1–5 received orally administered vaccine candidates. Group 1 received NC (300 μL). Group 2 received NP-Empty (without OmpA). Group 3 received OmpA (4 μg/g). Groups 4 and 5 received NP-OmpA (4 μg/g and 8 μg/g, respectively). Mice in Group 6 received intraperitoneal injections of NP-OmpA (4 μg/g). After 7 days of continuous oral administration, the serum and liver of the mice were taken. After homogenizing in ice-cold PBS, the liver tissues were centrifuged (900 g, 4°C, 10 min), and the supernatants were assayed for alanine aminotransferase (ALT), aspartate transaminase (AST), catalase (CAT), glutathione (GSH), malondialdehyde (MDA), and superoxide dismutase (SOD) using assay kits. Serum uric acid (UA) and creatinine (Cr) were measured according to the kit instructions (Jiancheng Institute of Biotechnology, China).

Determination of immune-related gene and inflammation-related gene expression by qRT-PCR

First, mRNA was isolated from the spleen, liver, and kidney tissues using an RNA isolation kit (TAKARA, Japan) and according to the manufacturer's instructions, as described previously [21]. Briefly, the mRNA was reverse-transcribed to cDNA using a PrimeScript RT Master Mix kit (TAKARA, Japan), and cDNAs were amplified using the primers shown in Table 1. The qRT-PCR was performed using an Applied Biosystems StepOnePlus™ Real-Time PCR System (ABI Applied Biosystems, USA) with a SYBR® Green Permix Pro Taq HS qPCR kit (TAKARA, Japan). The mRNA expression was analyzed by the $2^{-(\Delta\Delta Ct)}$ formula and GAPDH was included as an internal control gene.

Histopathological morphology of injury to visceral organs

The preparation of pathological sections of mice liver and kidney involved dehydration, transparency, sectioning, and H & E staining [21]. Briefly, the liver and kidney were dehydrated using an alcohol gradient for 1 h and then placed in an alcohol: xylene mixture (1:1, V/V) for 30 min, xylene for 8 min, xylene: paraffin solution (1:1, V/V) for 30 min, and paraffin for 1 h. Slices with a thickness of about 5 μm were cut, dried, H & E stained, observed under a microscope, and photographed (Leica, Germany).

Results

Expression and purification of recombinant OmpA

Recombinant OmpA was obtained using Ni-NTA super flow resin. It had a molecular weight of about 60 kDa, comprised of the 39 kDa OmpA and the 20 kDa fusion protein, as shown in Fig. 1.

Preparation of OmpA nanoparticles

The OmpA nanoparticles (NP-OmpA) were 700.8 ± 14.6 nm in size, and they had a uniform and spherical shape (Fig. 2), and the zeta potential was 33.06 ± 1.15 MV. The LE was 79.27%, and the LC was 20.31%.

The gastric environment was simulated using PBS (pH 1.2) to assess the OmpA release from the NP-OmpA. The release rate was fast from 0-48 h and then relatively slow from 48-96 h, and less than 50% (Fig. 3).

Optimal preparation conditions for NP-OmpA

The optimal preparation conditions for NP-OmpA were investigated by assessing the LE, LC, particle size, and morphology of the nanoparticles. The optimal concentration of OmpA was 2 mg/mL (Fig. 4A). Regarding CS, the LE and LC increased as the CS concentration rose from 1 mg/mL to 5 mg/mL, and the optimal CS concentration was 5 mg/mL (Fig. 4B), where LE and LC were 76.48% and 20.31%, respectively. The optimal ratio of TPP/CS (W/W) was 1:1, with LE of 78.37% and LC of 19.31% (Fig. 4C). The optimal magnetic mixing speed was 150 r/min, with LE of 76.59% and LC of 18.31% (Fig. 4D). The optimal mixing time was 15 min, with LE of 76.42% and LC of 19.86% (Fig. 4E).

Effect of NP-OmpA on mouse liver and kidney function

NP-OmpA safety was determined by examining the functional and antioxidant indexes of mice kidneys and livers. To investigate the kidney function index, serum UA and Cr were measured, and the results showed that there was no significant difference between animals immunized with NP-OmpA and with OmpA, NC, and NP-Empty (Fig. 5A and 5B). To investigate the liver function index, ALT and AST were measured, and no significant differences were found between the NP-OmpA group and control groups (Fig. 5C and 5D). The liver antioxidant index (CAT and GSH) showed no significant differences between any groups (Fig. 5E and 5F). The liver membrane lipid peroxidation index, determined using MDA measurements, showed no significant differences between any groups (Fig. 5G).

Histopathological observations of tissues from mice immunized with NP-OmpA

The liver sections showed that mice immunized with NP-OmpA and with control agents had obvious hepatic sinusoids and cells with regular cell morphology, uniform cytoplasm, and clear nuclei (Fig. 6A). The kidney sections showed that mice immunized with NP-OmpA and with control agents had normal glomerular morphology, renal tubules arranged in order, and no obvious congestion or edema in the renal interstitium (Fig. 6B).

Immuno-stimulating activity of NP-OmpA

The mRNA expression of immune-related genes in the spleen, liver, and kidney was detected by qRT-PCR. Compared with the NC and OmpA control groups, the NP-OmpA group (orally administered 8 μg/g) activated higher expression levels of IFN-γ and HSP70 in the spleen, liver, and kidney (Fig. 7A).

The mRNA expression of inflammation-related genes in spleen, liver, and kidney was detected after mice were challenged with *E. coli*. The results showed that the expression levels of TNF-a, IL-6, and IL-10 were decreased in the spleen, liver, and kidney compared with the control group, especially in the spleen (Fig. 7B).

Antioxidant-related factors were detected in the liver after challenge with *E. coli*. Animals immunized with NP-OmpA and OmpA had lower MDA and SOD liver levels than those that received NC. The level was lower in those immunized with NP-OmpA compared to those that received OmpA (Fig. 7C).

Regarding the thymus index, spleen index, and phagocytic percentage (*PP*), the measurements in the NP-OmpA group were higher than those of the other groups, and the thymus index reached significance ($p < 0.05$). The spleen index and *PP* of the NP-OmpA and OmpA groups were significant ($p < 0.05$) compared to the other groups (Table 2).

ELISA results showed that antibodies from mice immunized with NP-OmpA interacted with *E. coli* when the titer reached a 1:1600 dilution, which was higher than OmpA, NP-OmpA and NC groups (Fig. 8A). Mice immunized with NP-OmpA were found to have antibodies that bound to activated OmpA at a dilution of 1: 3200, which was a higher titer than mice immunized with OmpA, NP-Empty and NC (Fig. 8B).

Immunoprotective effect of NP-OmpA

Mice were orally immunized with NP-OmpA, OmpA, NP-Empty, and NC, respectively. The immunoprotective effect was evaluated by challenge with *E. coli*. Mice developed severe toxic symptoms that gradually improved after 4 days. The immune protection rate of NP-OmpA immunization (71.43%) was significantly higher ($P < 0.05$) than that of OmpA (28.57%), NP-Empty (7.14%), and NC (Table 3).

Liver and kidney histopathology of mice challenged with *E. coli*

Liver and kidney sections were prepared after *E. coli* challenge to observe any injury. Compared to the livers of mice immunized with NP-OmpA (orally administered 8 μg/g), OmpA, and negative control (without *E. coli* challenge), livers of mice that received NC appeared to have inflammatory cell infiltration in the central vein, nuclear apoptosis, and unclear hepatic sinuses after challenge (Fig. 9A), and the kidneys of mice received NC appeared to have glomerular atrophy (Fig. 9B). What's more, the livers and kidneys of mice immunized with NP-OmpA appeared to have less injury than those of mice immunized with OmpA.

Discussion

Nanomaterials exhibit specific properties or functions, which has attracted extensive attention in biomedicine. Active compounds can be coated with specific materials to prepare nanoparticles, and these coating materials can help to promote and maintain the biological activity of the encapsulated compounds, facilitate sustained release, change the method of administration, improve drug utilization, reduce adverse reactions, and can be degraded and absorbed by the host [22, 23]. When applied to oral

vaccines, nanoparticles can protect drugs from degradation by gastrointestinal enzymes, improve the bioavailability of drugs, and enhance drug function [24, 25]. CS is a natural amino polysaccharide resulting from the deacetylation of chitin and has high biodegradability and biocompatibility, making it useful in medicine, food, textiles, and so on [26, 27]. Khouloud et al. used CS to encapsulate whey protein and prepare whey-CS nanoparticles, and this formulation improved the stability of whey protein [28]. CS was used to synthesize immobilizing glucoamylase nanoparticles, which retained 80% activity after 4 months [29]. *Edwardsiella tarda* OmpA was encapsulated with CS, the post-challenge survival proportion (PCSP) was 73.3%, and the nanoparticles could enhance immunological function [30]. In this study, OmpA was purified by Ni-NTA slurry and encapsulated with CS to prepare NP-OmpA nanoparticles with diameters of about 700 nm. The optimal preparation conditions for NP-OmpA included an OmpA concentration of 2 mg/mL, a CS concentration of 5 mg/mL, a ratio of TPP/CS (W/W) of 1:1, a magnetic mixing speed of 150 r/min and a mixing time of 15 min. In acidic solution (pH 1.2), the release rate of the NP-OmpA was less than 50%, indicating that NP-OmpA were stable in gastric juice. Thus, NP-OmpA could survive degradation in the gastrointestinal tract and may have value in oral delivery applications.

Internalized NP-OmpA may affect the host's health; therefore, it is necessary to evaluate visceral organ function and injury. UA and Cr levels were mainly used to determine kidney function indexes, and ALT, AST, CAT, GSH, and MDA levels were used to detect liver function. Using the levels of MPO, SOD, MDA, GSH-Px, GSH, and MDA, and immunohistochemical and immunofluorescence analyses, Lu et al. evaluated the protective effects of dexmedetomidine on lipopolysaccharide induced acute lung injury [31], and Ezz-Eldin et al. assessed the possible protective effect of carvacrol against bronchial asthma induced experimentally in rats [32]. Alhusaini et al. found that the intake of N-acetylcysteine (NAC) and thymoquinone (THQ) could protect against the nephrotoxicity induced by sodium fluoride (NAF) by analyzing SOD, GSH, UA, and Cr [33]. Our results showed that there were no significant differences in serum UA and Cr, in liver ALT, AST, CAT, GSH, and MDA, or in liver and kidney sections between mice immunized with NP-OmpA and the control group. These results suggest that NP-OmpA have no toxic effect on mice livers and kidneys.

Animals can be immunized with protegrin to enhance immune function and increase resistance to pathogen infection [34, 35]. This study found that NP-OmpA could significantly increase the immune-related gene expression of IFN-γ and HSP70, and the phagocytic activity to *S. aureus* of WBC in mice, which showed that the non-specific immune function was enhanced [36]. *S. aureus* is also a major causative agent of cow mastitis [1], and immunization with NP-OmpA may boost resistance to *S. aureus* infection. Moreover, we found that antiserum from animals immunized with NP-OmpA interacts with *E. coli*, which suggests that anti-NP-OmpA antibodies and *E. coli* formed antigen-antibody complexes and likely enhanced antigen presentation [15]. Also, antibodies from mice immunized with NP-OmpA bound to OmpA at a higher titer (1: 3200) than those from mice immunized with OmpA. This suggests that NP-OmpA can enhance the immune activity of mice.

The immune protection function of the protein against bacterial infection can be evaluated by immunizing mice with the protein and challenging the mice with the pathogenic bacteria, and then

analyzing the death rate [16], visceral organ injury [37], and expression of inflammation-related genes and antioxidant factors [38, 39]. Our study showed that the immune protection effect of NP-OmpA was 71.43% ($P < 0.05$), which was higher than that of OmpA (28.57%), NP-Empty (7.14%), and the NC group. After mice were challenged with *E. coli*, immunization with NP-OmpA was shown to decrease the expressions of the inflammation-related genes TNF-a, IL-6, and IL-10, and the expression of antioxidant factors MDA and SOD was also decreased, which indicated that immunization with NP-OmpA could reduce the inflammatory reaction caused by *E. coli*. Moreover, examination of histopathological sections showed that immunization with NP-OmpA could reduce injury to mice livers and kidneys caused by *E. coli*. These results suggest that NP-OmpA confer an immune protection against *E. coli* infection in mice.

Conclusions

Novel nanoparticles (NP-OmpA) were synthesized, and the preparation method was optimized. The detection of antioxidant factors and histopathological observation confirmed that the NP-OmpA was safe for mice and the immune protection rate was 71.43% ($P < 0.05$). Immunization with NP-OmpA could enhance the expression of immune factors and leukocyte phagocytosis of *S. aureus.* A high antiserum titer was obtained from mice immunized with NP-OmpA, and antibodies recognized *E. coli*. NP-OmpA could down-regulate the expression of inflammation-related genes and antioxidant factors and reduce visceral organ injury induced by *E. coli*. This study contributes to the development of an orally delivered nanoparticle that can be used to boost resistance to infection with the pathogenic bacteria that cause cow mastitis.

Declarations

Acknowledgements

Not applicable.

Authors' contributions

XL, XYZ and CC designed the experiment. XL, NNW and WS were involved in the animal experimentation. SJJ and CLC were involved in the sample analysis. The manuscript was edited by XL, NNW and XYZ. All authors read and approved the final manuscript.

Funding

This work was supported by the Key Research and Development Program of Shaanxi (2020LSFP2-38) and Project of Shaanxi University of Technology (SLGQD1803), China.

Availability of data and materials

The data were shown in the main manuscript and supplemental materials.

Ethics approval and consent to participate

All procedures of this study were reviewed and approved by the Animal Ethics Committee of the Shaanxi University of Technology (2019-015).

Consent for publication

Not applicable.

Competing interests

The authors declare that they have no competing interests.

Author details

[1]College of Veterinary Medicine, Northwest A&F University, Yangling 712100, China. [2]Chinese-German joint Institute for natural product research, College of Biological Science and Engineering, Shaanxi University of Technology, Hanzhong 723000, China

References

1. Askari N, Ghanbarpour R. Molecular investigation of the colicinogenic *Escherichia coli* strains that are capable of inhibiting *E. coli* O157: H7 in vitro. BMC Vet Res. 2019;15(1):14.
2. Fazel F, Jamshidi A, Khoramian B. Phenotypic and genotypic study on antimicrobial resistance patterns of *E. coli* isolates from bovine mastitis. Microb Pathog. 2019;132:355–61.
3. Lavon Y, Leitner G, Kressel Y, Ezra E, Wolfenson D. Comparing effects of bovine *Streptococcus* and *Escherichia coli* mastitis on impaired reproductive performance. J Dairy Sci. 2019;102(11):10587–98.
4. Belotserkovsky I, Sansonetti PJ. Shigella and enteroinvasive *Escherichia coli*. Curr Top Microbiol Immunol. 2018;416:1–26.
5. Sheen S, Huang CY, Ramos R, Chien SY, Scullen OJ, Sommers C. Lethality prediction for *Escherichia coli* O157: H7 and uropathogenic *E. coli* in ground chicken treated with high pressure processing and trans-cinnamaldehyde. J Food Sci. 2018;83(3):740–9.
6. Wassenaar TM. *E. coli* and colorectal cancer: a complex relationship that deserves a critical mindset. Crit Rev Microbiol. 2018;44(5):619–32.
7. Rowley CA, Anderson CJ, Kendall MM. Ethanolamine influences human commensal *Escherichia coli* growth, gene expression, and competition with enterohemorrhagic *E. coli* O157: H7. mBio. 2018;9(5):e01429–18.

8. Zhao WD, Liu DX, Wei JY, Miao ZW, Zhang K, Su ZK, et al. Caspr1 is a host receptor for meningitis-causing *Escherichia coli*. Nat Commun. 2018;9(1):2296.
9. Castillo JI, Równicki M, Wojciechowska M, Trylska J. Antimicrobial synergy between mRNA targeted peptide nucleic acid and antibiotics in *E. coli*. Bioorg Med Chem Lett. 2018;28(18):3094–8.
10. Roth N, Käsbohrer A, Mayrhofer S, Zitz U, Hofacre C, Domig KJ. The application of antibiotics in broiler production and the resulting antibiotic resistance in *Escherichia coli*: a global overview. Poult Sci. 2019;98(4):1791–804.
11. Confer AW, Ayalew S. The OmpA family of proteins: roles in bacterial pathogenesis and immunity. Vet Microbiol. 2013;163(3-4):207-22.
12. Boags AT, Samsudin F, Khalid S. Binding from both sides: TolR and full-length OmpA bind and maintain the local structure of the *E. coli* cell wall. Structure. 2019;27(4):713–24.
13. Hsieh WS, Yang YY, Lin PH, Chang CC, Wu HH. Recombinant OmpA protein fragments mediate interleukin-17 regulation to prevent *Escherichia coli* meningitis. J Microbiol Immunol Infect. 2016;49(6):843–50.
14. Gu H, Liao Y, Zhang J, Wang Y, Liu Z, Cheng P, et al. Rational design and evaluation of an artificial *Escherichia coli* K1 protein vaccine candidate based on the structure of OmpA. Front Cell Infect Microbiol. 2018;8:172.
15. Chen C, Wu NN, Rong N, Kang C, Chen CL, Wu SQ, et al. Immunoprotective evaluation of *Escherichia coli* outer membrane protein A against the main pathogens of animal mastitis. Trop J Pharm Res. 2020;19 (1):155–62.
16. Liu X, Yang MJ, Wang SN, Xu D, Li H, Peng XX. Differential antibody responses to outer membrane proteins contribute to differential immune protections between live and inactivated *Vibrio parahemolyticus*. J Proteome Res. 2018;17(9):2987–94.
17. Li XY, Kong XY, Shi S, Zheng XL, Guo G, Wei YQ, et al. Preparation of alginate coated chitosan microparticles for vaccine delivery. BMC Biotechnology. 2008;8:89–100.
18. Marslin G, Prakash J, Qi SS, Franklin G. Oral delivery of curcumin polymeric nanoparticles ameliorates CCl□-induced subacute hepatotoxicity in wistar rats. Polymers (Basel). 2018;10(5):541–52.
19. Liu X, Chen CL, Chen C, Marslin Gregory, Ding Rui, Wu SQ. Construction and evaluation of a novel triple cell epitope-based polypeptide vaccine against cow mastitis induced by *Staphylococcus aureus*, *Escherichia coli* and *Streptococcus*. Trop J Pharm Res. 2017;16(10):2477–86.
20. Meehan TL, Yalonetskaya A, Joudi TF, McCall K. Detection of cell death and phagocytosis in the drosophila 0vary. Methods Mol Biol. 2015;1328:191–206.
21. Liu X, Chen C, Zhang XY. Drug-drug interaction of acetaminophen and roxithromycin with the cocktail of cytochrome P450 and hepatotoxicity in rats. Int J Med Sci. 2020;17(3):414–21.
22. Paunovska K, Loughrey D, Sago CD, Langer R, Dahlman JE. Using large datasets to understand nanotechnology. Adv Mater. 2019;31(43):e1902798.

23. Song W, Anselmo AC, Huang L. Nanotechnology intervention of the microbiome for cancer therapy. Nat Nanotechnol. 2019;14(12):1093–103.
24. Xu C, Yang S, Jiang Z, Zhou J, Yao J. Self-propelled gemini-like LMWH-scaffold nanodrugs for overall tumor microenvironment manipulation via macrophage reprogramming and vessel normalization. Nano Lett. 2020;20(1):372–83.
25. Zhang Y, Wang L, Xu M, Zhao T, Kuang L, Hua D. Smart oral administration of polydopamine-coated nanodrugs for efficient attenuation of radiation-induced gastrointestinal syndrome. Adv Healthc Mater. 2020;9(13):e1901778.
26. Muxika A, Etxabide A, Uranga J, Guerrero P, de la Caba K. Chitosan as a bioactive polymer: Processing, properties and applications. Int J Biol Macromol. 2017;105(2):1358–68.
27. Zhang E, Xing R, Liu S, Qin Y, Li K, Li P. Advances in chitosan-based nanoparticles for oncotherapy. Carbohydr Polym. 2019;222:115004.
28. Matias LLR, Costa ROA, Passos TS, Queiroz JLC, Serquiz AC, Maciel BLL, et al. Tamarind trypsin inhibitor in chitosan-wheyprotein nanoparticles reduces fasting blood glucose levels without compromising insulinemia: a preclinical study. Nutrients. 2019;11(11): 2770.
29. Wang DQ, Jiang WF. Preparation of chitosan-based nanoparticles for enzyme immobilization. Int J Biol Macromol. 2019;126:1125–32.
30. Dubey S, Avadhani K, Mutalik S, Sivadasan SM, Maiti B, Girisha SK, et al. *Edwardsiella tarda* OmpA encapsulated in chitosan nanoparticles shows superior protection over inactivated whole cell vaccine in orally vaccinated fringed-Lipped *Peninsula Carp* (Labeo fimbriatus). Vaccines (Basel). 2016;4(4):40.
31. Lu M, Li LY, Lu S, Li K, Su Z, Wang Y, et al. The protective effect of dexmedetomidine on LPS-induced acute lung injury through the HMGB1- mediated TLR4/NF-κB and PI3K/Akt/mTOR pathways. Mol Immunol. 2018;94:7–17.
32. Ezz-Eldin YM, Aboseif AA, Khalaf MM. Potential anti-inflammatory and immunomodulatory effects of carvacrol against ovalbumin-induced asthma in rats. Life Sci. 2020;242:117222.
33. Alhusaini AM, Faddah LM, El Orabi NF, Hasan IH. Role of some natural antioxidants in the modulation of some proteins expressions against sodium fluoride-induced renal injury. Biomed Res Int. 2018;2018:5614803.
34. Benfaremo D, Manfredi L, Luchetti MM, Gabrielli A. Musculoskeletal and rheumatic diseases induced by immune checkpoint inhibitors: a review of the literature. Curr Drug Saf. 2018;13(3):150–64.
35. Aaby P, Benn CS. Developing the concept of beneficial non-specific effect of live vaccines with epidemiological studies. Clin Microbiol Infect.2019;25(12): 1459–67.
36. Chaudhury A, Noiret L, Higgins JM. White blood cell population dynamics for risk stratification of acute coronary syndrome. Proc Natl Acad Sci. 2017;114(46):12344–9.
37. Solana JC, Ramírez L, Cook EC, Hernández-García E, Sacristán S, Martín ME, et al. Subcutaneous immunization of *Leishmania* HSP70-II null mutant line reduces the severity of the experimental visceral leishmaniasis in BALB/c mice. Vaccines. 2020;8(1):141.

38. Zhang XM, Zhao HL, Wang JJ, Liao Y, Na RX, Wang LC, et al. Evaluation of immune responses and related patho-inflammatory reactions of a candidate inactivated EV71 vaccine in neonatal monkeys. Zhonghua Yi Xue Za Zhi. 2011;91(28):1977–81.
39. Santos KO, Costa-Filho J, Riet J, Spagnol KL, Nornberg BF, Kütter MT, et al. Probiotic expressing heterologous phytase improves the immune system and attenuates inflammator response in zebrafish fed with a diet rich in soybean meal. Fish Shellfish Immun. 2019;93:652–8.

Tables

Table 1 Primers used for qRT-PCR

Gene	Forward primer (5'-3')	Reverse primer (5'-3')
IFN-γ	TCAAGTGGCATAGATGTGGAAGAA	TGGCTCTGCAGGATTTTCATG
HSP70	GAAGGTGCTGGACAAGTGC	GCCAGCAGAGGCCTCTAATC
TNF-a	TATGGCTCAGGGTCCAACTC	GCTCCAGTGAATTCGGAAAG
IL-6	GACAAAGCCAGAGTCCTTCAGAGAGATACAG	TTGGATGGTCTTGGTCCTTAGCCAC
IL-10	AACATACTGCTAACCGACTC	ATGCTCCTTGATTTCTGG
GAPDH	ACAGTCCATGCCATCACTGCC	GCCTGCTTCACCACCTTCTTG

Table 2 WBC, organ index, and leukocyte phagocytosis of *S. aureus* values

Group	Compound	WBC no. ($\times 10^9$/L)	Thymus index	Spleen index	Phagocytic percentage (*PP* %)	Phagocytic index (*PI*)
1	NP-OmpA	6.83±0.97a	2.67±0.12b	4.67±0.38b	5.76±1.10b	3.56±0.62a
2	Control 1 (OmpA)	6.93±0.89a	2.25±0.10a	4.01±0.41ab	4.85±0.33ab	3.67±0.42a
3	Control 2 (NP-Empty)	6.73±0.48a	2.08±0.07a	3.48±0.43a	4.68±1.02a	3.08±0.43a
4	Control 3 (Normal saline)	6.68±0.67a	2.03±0.11a	3.31±0.25a	4.21±0.98a	3.16±0.58a

Labels a–b indicate statistically different groups ($P < 0.05$). Mice immunized with NP-OmpA recorded higher thymus index, spleen index, and *PP* values than other groups, indicating that NP-OmpA have immuno-stimulating activity.

Table 3 Active immune protection achieved in mice

Group	Compound	Nos	Survival no.	Death no.	ADR, %	RPS, %
1	NP-OmpA	15	11	4	26.67	71.43**
2	Control 1 (OmpA)	15	5	10	66.67	28.57
3	Control 2 (NP-Empty)	15	2	13	86.67	7.14
4	Control 3 (Normal saline)	15	1	14	93.33	—

Notes: ADR, accumulating death rates. RPS, immune protection rate. RPS (%) = 1 - (% vaccinated mortality/% non-vaccinated mortality) × 100. ** $P < 0.01$ (compared with control 3). The highest RPS was in the NP-OmpA-immunized group (71.43%), followed by the OmpA-immunized group (28.57%), while the NP-Empty-immunized group (7.14%) had the lowest RPS. There was a significant difference ($P < 0.05$) between groups immunized with NP-OmpA and with OmpA, NP-Empty and NC.

Figures

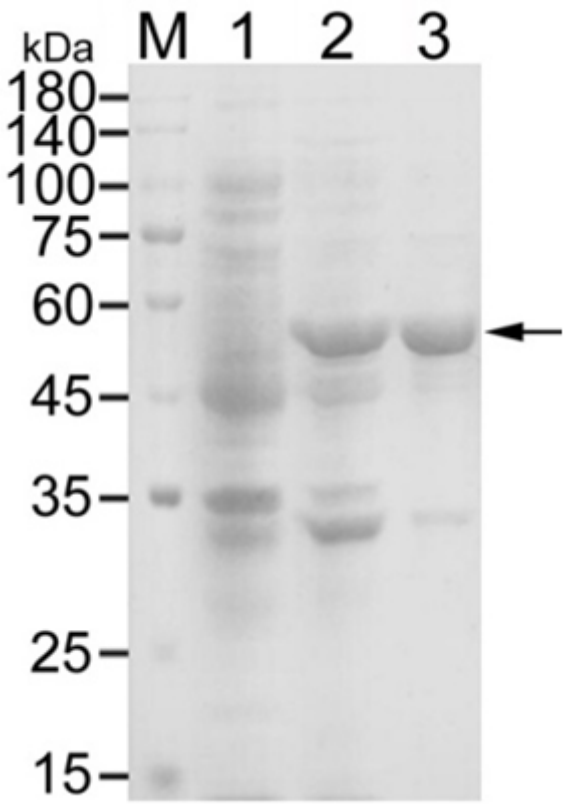

Figure 1

Purification of OmpA. M, protein marker; 1, non-induced strain; 2, IPTG-induced strain; 3, purified OmpA.

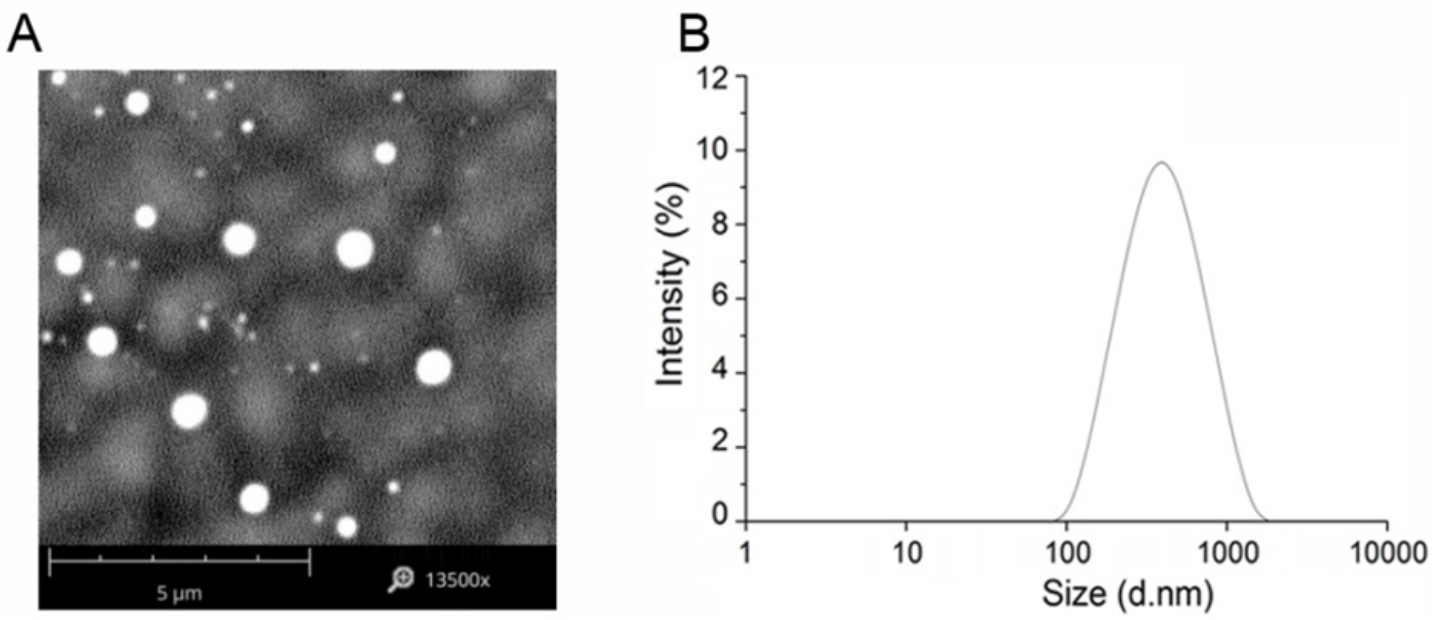

Figure 2

Morphology and particle size distribution of NP-OmpA. A, scanning electron micrograph of NP-OmpA; B, particle size distribution of NP-OmpA. The surface morphology and size distribution of NP-OmpA was uniform and spherical, and the particle size was about 700 nm.

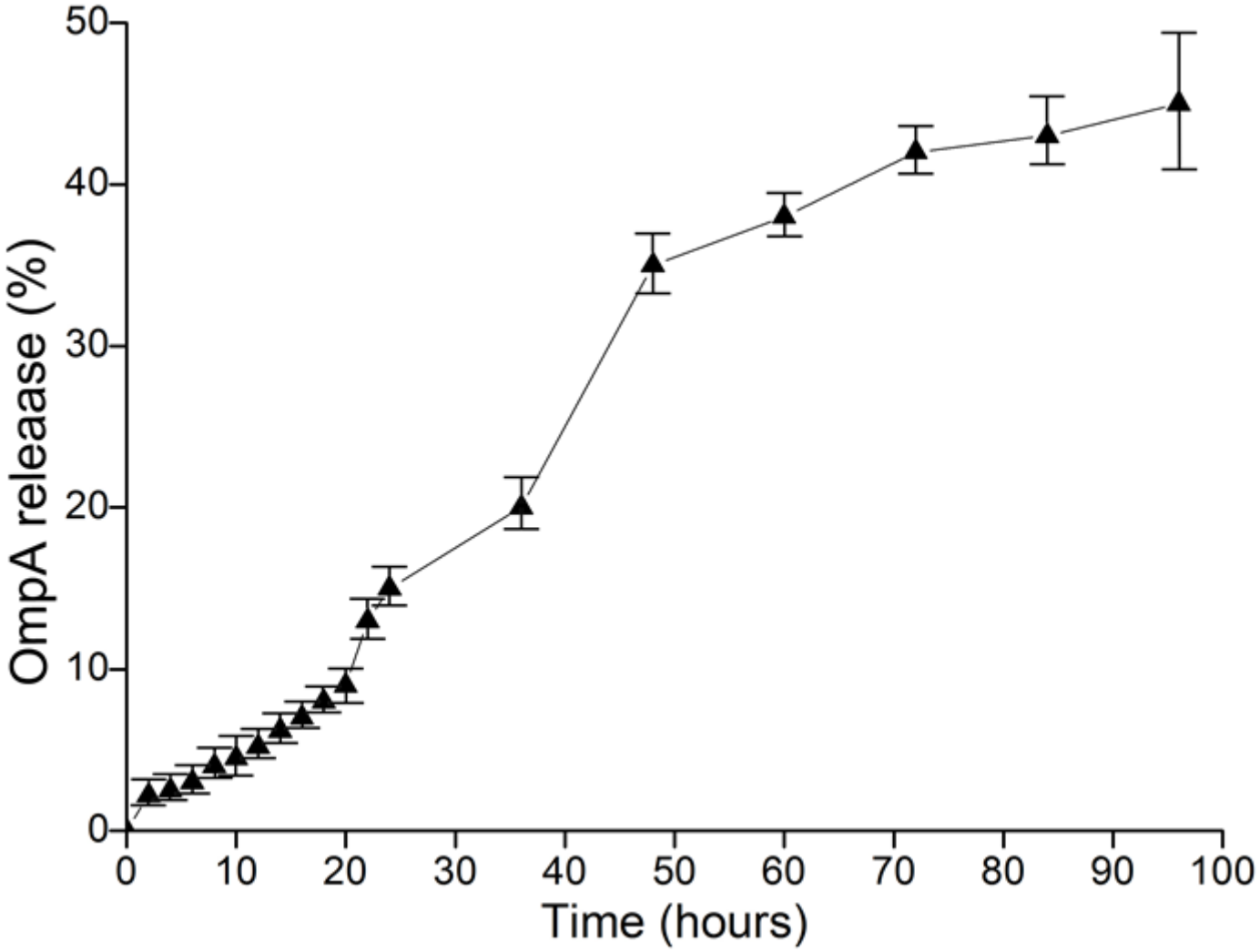

Figure 3

Characteristics of OmpA release from NP-OmpA in PBS (pH 1.2). The major release occurred from 0 to 48 h, and the release rate was < 50%.

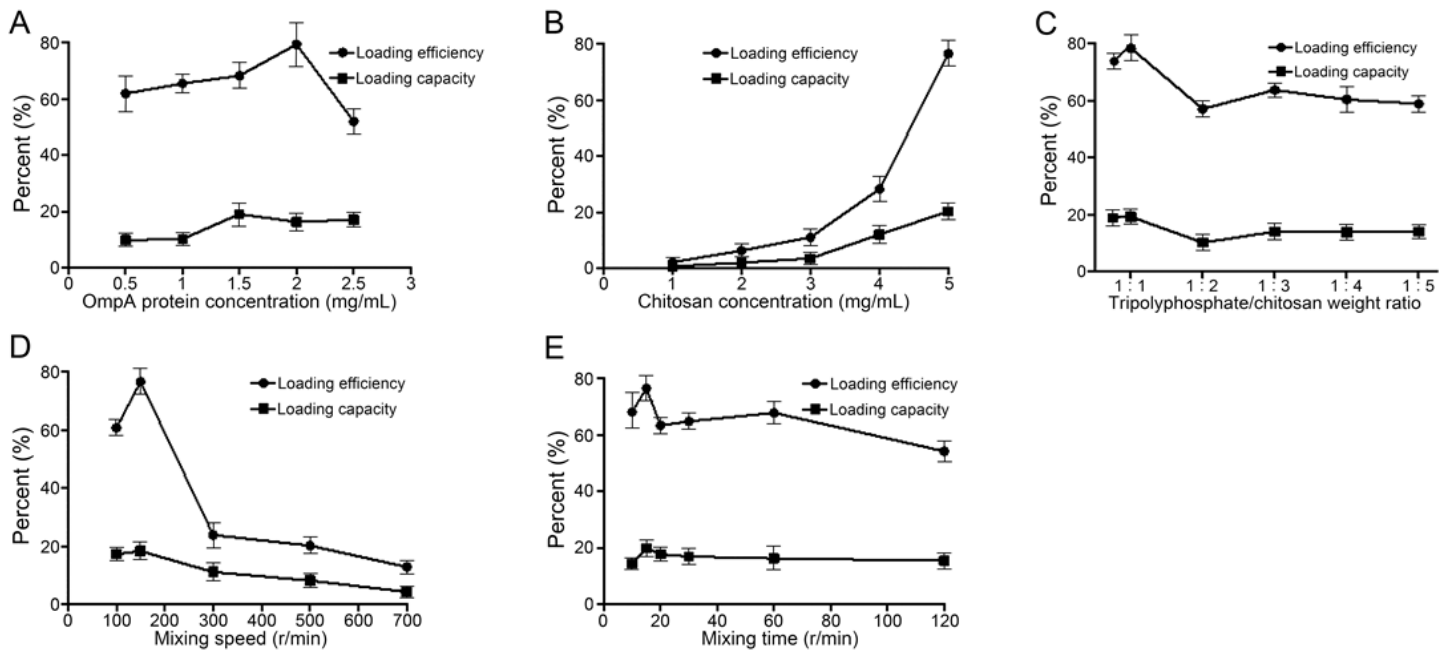

Figure 4

Effects of different factors on the preparation of NP-OmpA nanoparticles. A, the optimal concentration of OmpA was 2 mg/mL; B, the optimal concentration of CS was 5 mg/mL; C, the optimal ratio of TPP/CS (W/W) was 1:1; D, the optimal magnetic mixing speed was 150 r/min; E, the optimal mixing time was 15 min.

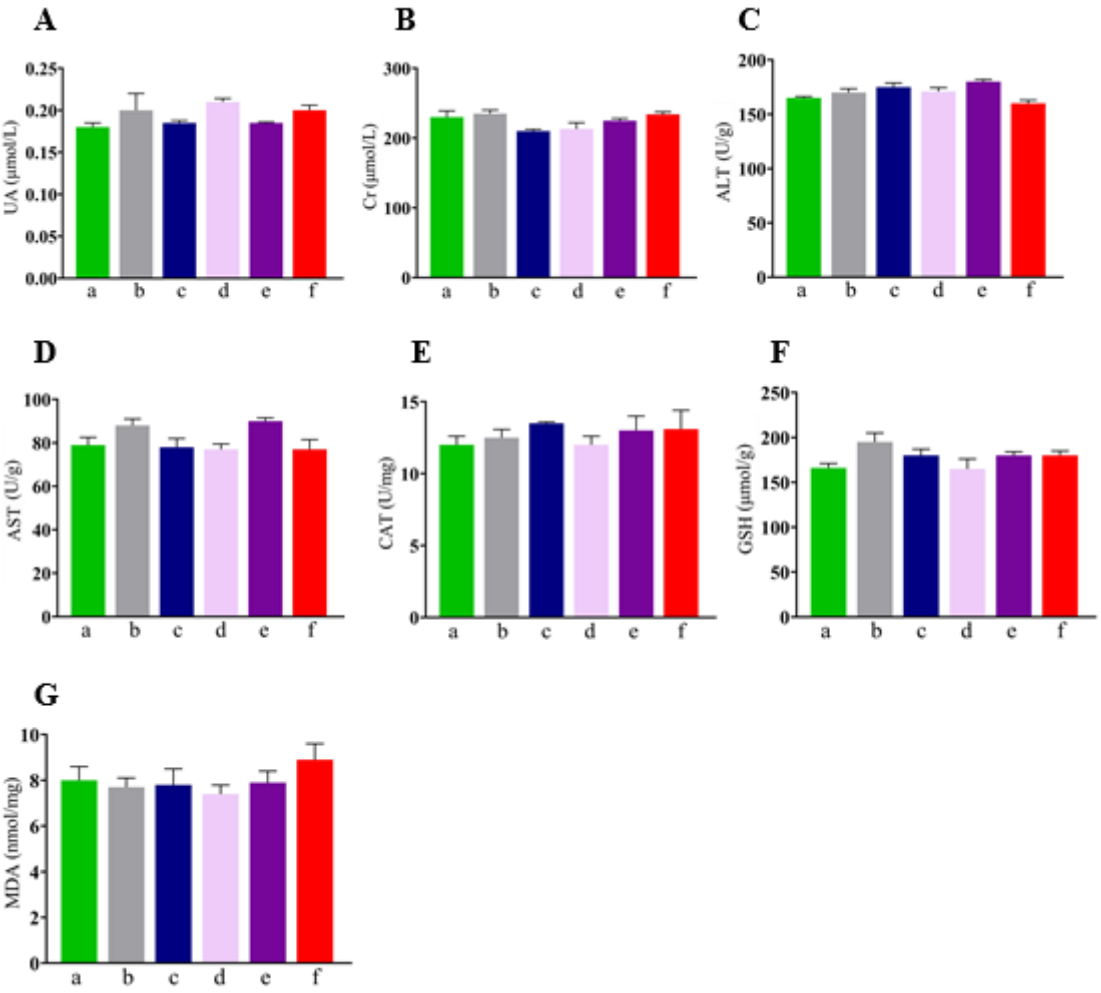

Figure 5

Effects of NP-OmpA immunization on liver and kidney functions in mice. A, B: Serum UA and Cr were measured to investigate kidney function. C, D: Liver ALT and AST were measured to investigate liver function. E, F: Liver CAT and GSH were measured to determine the liver antioxidant index. G: MDA was measured to determine the liver membrane lipid peroxidation index. Results of oral administration of NC (a), NP-Empty (b), 4 μg/g OmpA (c), 4 μg/g NP-OmpA (d), 8 μg/g NP-OmpA (e), and intraperitoneal injection of 4 μg/g NP-OmpA (f) are shown. There was no significant difference in UA, Cr, ALT, AST, CAT, GSH, and MDA between the NP-OmpA group and the other groups.

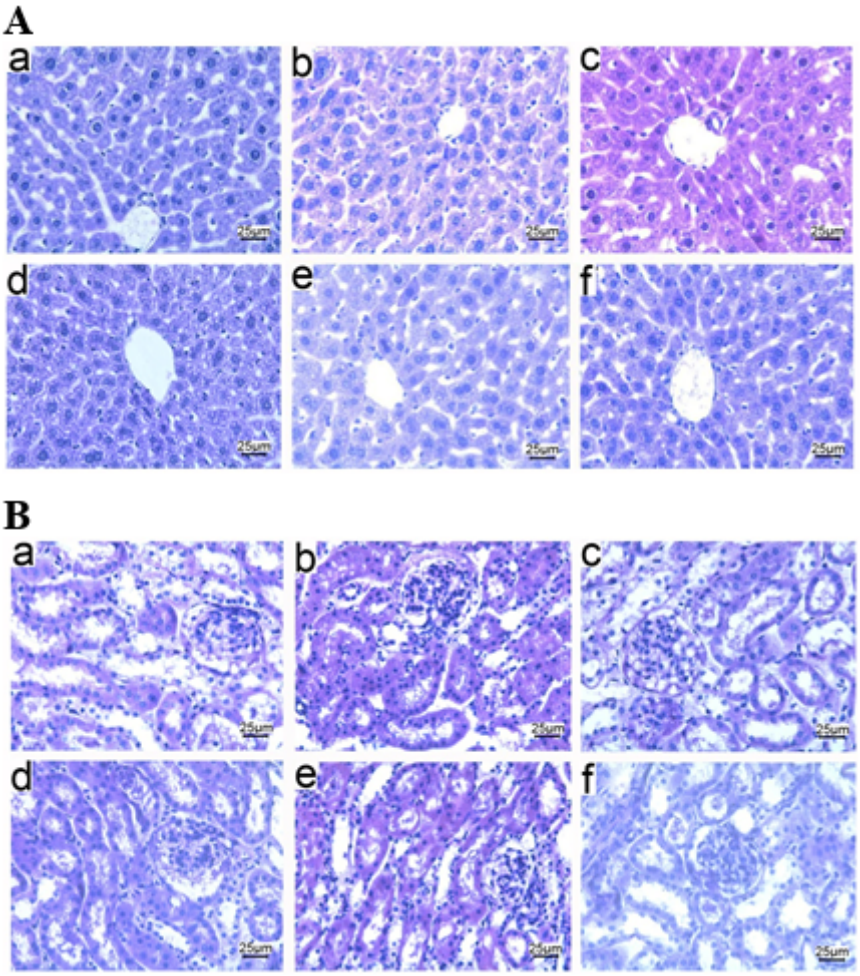

Figure 6

Histopathology of livers and kidneys of immunized mice. Liver (A) and kidney (B) sections are shown with H & E staining at × 400 magnification. Results of oral administration of NC (a), NP-Empty (b), 4 μg/g OmpA (c), 4 μg/g NP-OmpA (d), 8 μg/g NP-OmpA (e), and intraperitoneal injection of 4 μg/g NP-OmpA (f) are shown. Liver sections (A) show that every group had obvious hepatic sinusoids and cells with regular cell morphology, uniform cytoplasm, and clear nuclei. Kidney sections (B) show that every group had normal glomerular morphology, renal tubules arranged in order, and no obvious congestion or edema in the renal interstitium. The results showed that NP-OmpA had no toxic effect on mice livers and kidneys.

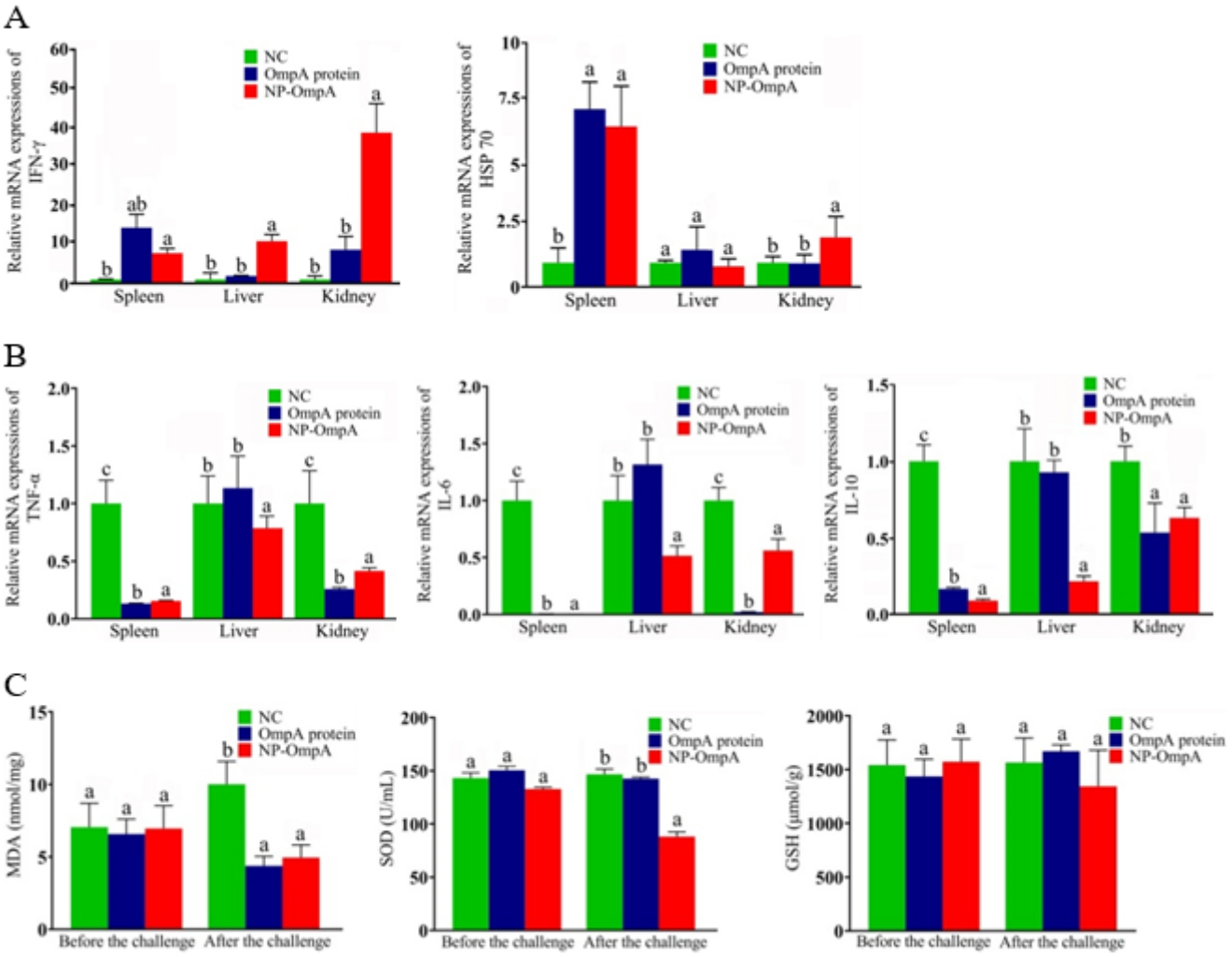

Figure 7

Analysis of immune-related factors before and after pathogenic E. coli challenge in mice. Labels a–c indicates statistically different groups ($P < 0.05$). (A) Effect of NP-OmpA on mRNA expression of immune-related factors before challenge. Compared to NC and OmpA, NP-OmpA activated higher expression levels of IFN-γ and HSP70 in the spleen, liver, and kidney. (B) Effect of NP-OmpA on mRNA expression of inflammation-related factors after challenge. Compared to NC, NP-OmpA and OmpA resulted in decreased expression levels of TNF-a, IL-6, and IL-10 in the spleen, liver, and kidney, especially in the spleen. (C) Levels of antioxidant-related factors before and after E. coli challenge. After challenge, animals immunized with NP-OmpA and OmpA had lower MDA and SOD liver levels than those that received NC, and the level was lower in those immunized with NP-OmpA compared to OmpA.

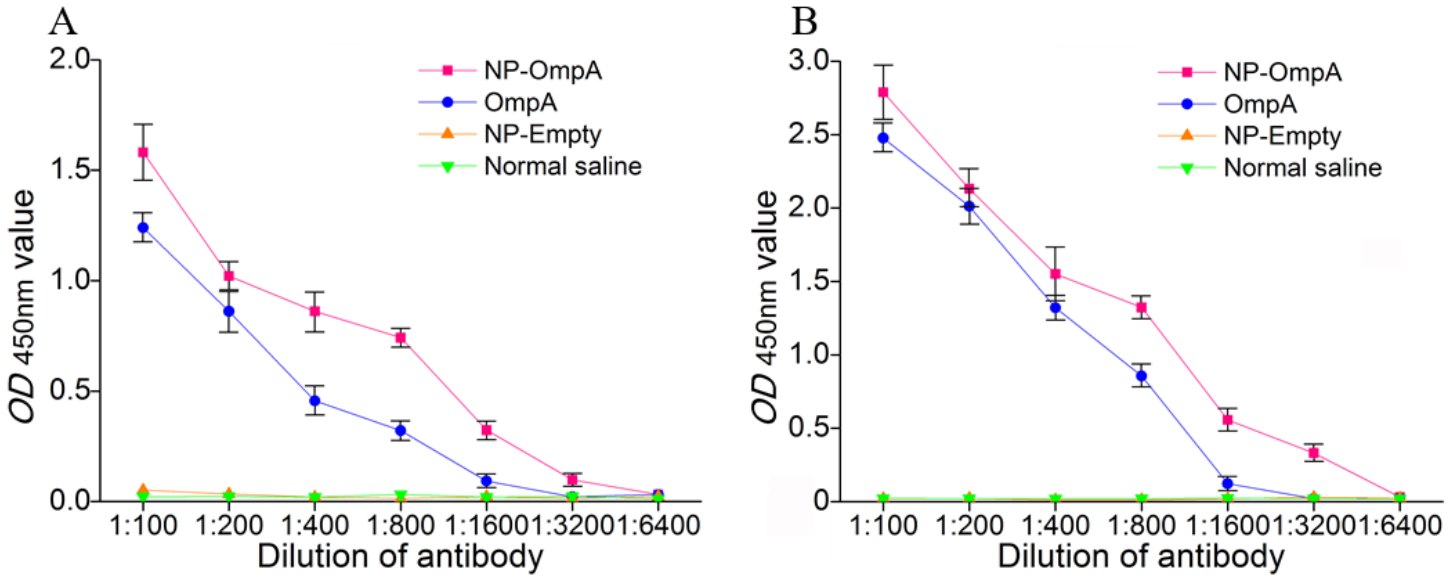

Figure 8

ELISA results showing the interaction between antibodies and E. coli (A) and antibody titer (B). Panel A shows that antibody from mice immunized with NP-OmpA interacted with E. coli when the titer reached a 1: 1600 dilution, and the binding ability of antibody from mice immunized with NP-OmpA to E. coli was greater than that of antibody from other groups in vitro. Panel B shows that antibody from mice immunized NP-OmpA bound to OmpA at a dilution of 1: 3200, a higher titer than other groups.

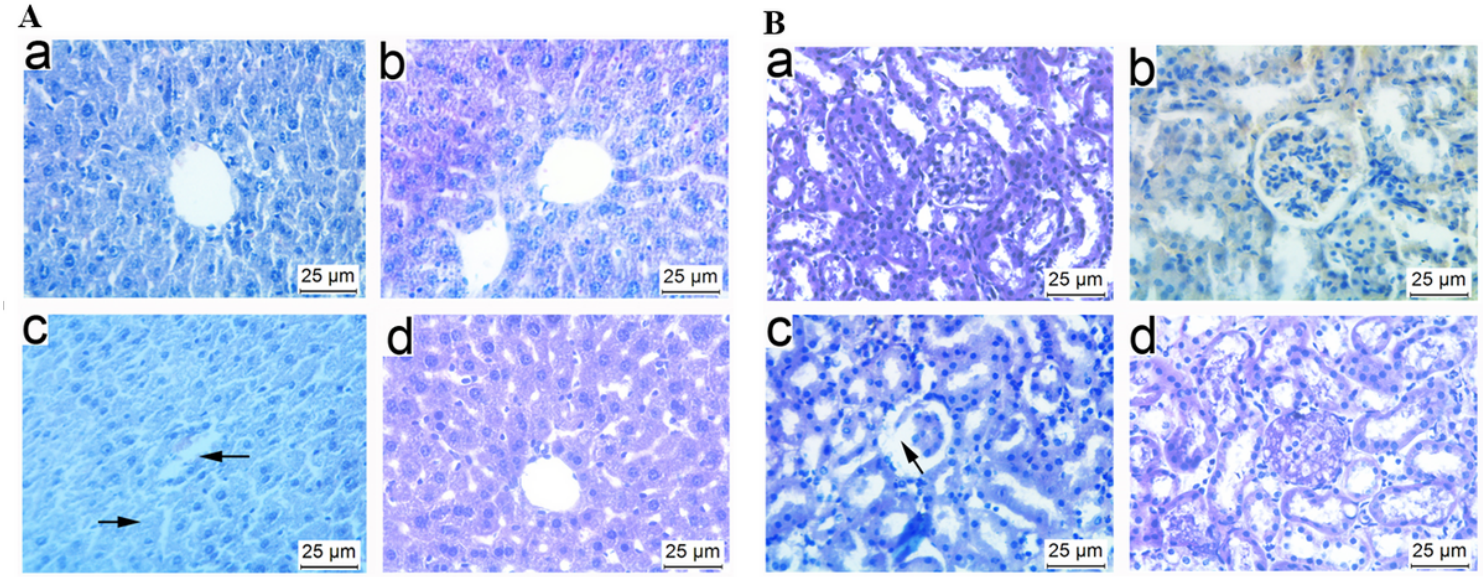

Figure 9

Histopathology of livers and kidneys of mice after immunization and E. coli challenge. Liver (A) and kidney (B) sections are shown with H & E staining at × 400 magnification. Mice were immunized with NP-OmpA (a), OmpA (b), or NC (c) and then challenged with E. coli, or immunized with NC and challenged with NC (d). Inflammatory cell infiltration in the central vein, nuclear apoptosis of liver cells, and unclear

hepatic sinuses are seen after E. coli challenge (Ac). Glomerular atrophy is seen after E. coli challenge (Bc). Thus, immunization with NP-OmpA can reduce the injury to the liver and kidney caused by E. coli.